Cytoskeletal Architecture and Organelle Transport in Giant Syncytia Formed by Fusion of Hexactinellid Sponge Tissues

SALLY P. LEYS

Department of Biology, University of Victoria, Victoria, British Columbia V8W 2Y2, Canada

Abstract. Dissociated tissue from the hexactinellid sponge *Rhabdocalyptus dawsoni* adheres to coated substrates and aggregates by the fusion of tissue pieces to form a giant syncytium. Video microscopy shows that the pieces contact each other by way of lamellipodia or filopodia. Fusion, corroborated by evidence of dye spread, occurs about 1 hour after plating and is characterized by two-way transport of individual organelles, including nuclei, at an average rate of 2.15 μm · s^{-1}, and bulk streaming of cytoplasm at an average velocity of 1.72 μm · s^{-1}. In the cellular sponge *Haliclona*, by contrast, dye does not spread through aggregates and no streaming can be seen. That transport in *Rhabdocalyptus* is microtubule-based is indicated by the reversible inhibition of streaming caused by colcemid and nocodazole. Immunofluorescence and electron microscopy reveal an extensive network of microtubule bundles within the aggregates. The cytoskeleton also includes microfilament bundles that traverse aggregates and run around the periphery and giant, actin-dense rods that extend from the edges. Cytochalasin B reversibly disrupts the microfilamentous framework without blocking streaming.

In contrast to demosponges where the cytoskeleton is organized on the basis of individual cells, in hexactinellids it provides a supporting framework and transport pathways within vast, multinucleate tissue masses. If we take this preparation as a model for tissue organization in the intact sponge, these findings support the view that hexactinellids are syncytial organisms, probably the largest in the animal kingdom, and suggest that food products may be distributed through the sponge intracellularly rather than by wandering amoebocytes. The findings strengthen the case for establishing the Hexactinellida as a subphylum within the Porifera.

Introduction

The syncytial organization of hexactinellid sponge tissue has been in question since the histology of dredged specimens was first examined. These animals, commonly known as glass sponges because of their siliceous skeleton, inhabit deep waters throughout the world's oceans, making their retrieval in good condition difficult. Early sponge researchers reported that there were no discernible membrane boundaries between nuclei (Schulze, 1887; Ijima, 1901). Although two cell types, archaeocytes and thesocytes, could be distinguished, most of the sponge was thought to be syncytial. At the time, however, many animal tissues were considered to be syncytial, including the pinacoderm of demosponges (Hyman, 1940), but phase contrast and electron microscopy have since revealed their cellular nature. Thus, the idea that hexactinellids were syncytial animals received little serious attention from modern sponge workers until recently.

Reiswig (1979) investigated hexactinellid histology using several populations accessible by scuba on the coast of British Columbia, Canada. Although his first attempts at electron microscopy with *Aphrocallistes vastus* and *Chonelasma calyx* were thwarted by difficulties with ultrastructural preservation, Reiswig nonetheless found no evidence to contradict Schulze's and Ijima's conclusions. Perseverance with electron microscopy with *Rhabdocalyptus dawsoni* (Fig. 1a) resulted in an improved fixation technique that provided ultrastructural evidence for two kinds of reticular, multinucleate tissues, the trabecular syncytium and the choanosyncytium, and for several types of cells (Mackie and Singla, 1983) (Fig. 1b). Most inter-
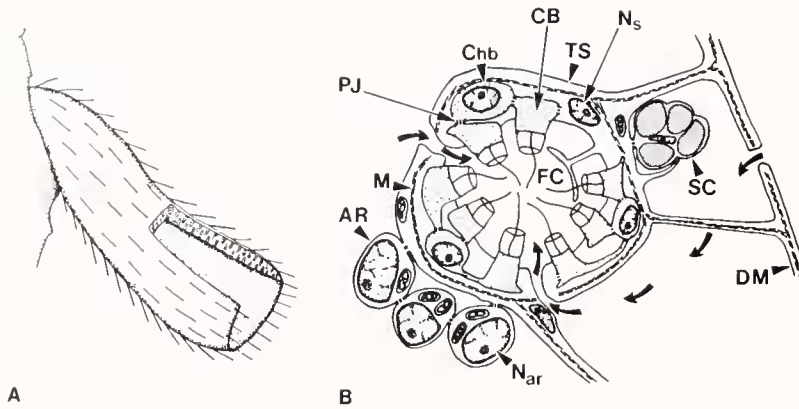
Figure 1. (A) Drawing of the hexactinellid sponge *Rhabdocalyptus dawsoni* with its osculum partially cut open. (B) Diagram illustrating the tissues of whole sponges. Water flows into choanoflagellate chambers (FC) as shown by the curved arrows, and is pumped out directly up from the center of the chamber. Trabecular syncytium (TS), collar body (CB), choanoblast (Chb), plugged junction (PJ), mesohyl (M), dermal membrane (DM), nucleus in the syncytium (N_s), nucleus of an archaeocyte (N_{ar}), spherulous cell (SC), archaeocyte (AR).

estingly, the syncytial cytoplasm was found to be connected to cellular components either by open cytoplasmic bridges or by a unique osmiophilic perforated plugged junction (Mackie, 1981). Sclerocytes were the only cell type not connected by plugs to the syncytium.

Concurrent electrophysiological studies with *Rhabdocalyptus* showed that following mechanical or electrical stimulation this sponge was capable of propagating signals at a rate of $0.26 \text{ cm} \cdot \text{s}^{-1}$ that stopped the flow of feeding currents throughout the whole animal, presumably by causing flagellar arrest (Lawn *et al.*, 1981; Mackie *et al.*, 1983). Because no nerves could be found, the syncytial tissues were proposed as the pathways for conduction, though no recordings of propagated electrical signals could be obtained.

Plugged junctions have since been reported in five of the six hexactinellids examined by electron microscopy, the exception being *Dactylocalyx pumiceus* (Reiswig, 1991). In this animal, no such junctions were found, but their presence could not be completely ruled out. Because of the remarkable differences in cellular organization between hexactinellids and other sponges and the physiological evidence of signal conduction, it was proposed that this group be separated from cellular sponges at the subphylum level (Reiswig and Mackie, 1983). Nonetheless, conclusive proof of syncytial organization from dye exchange experiments or from observations of cytoplasmic movements in living tissues has not been obtained, and recent investigations have raised doubts about the syncytial nature of hexactinellid larvae (Boury-Esnault and Vacelet, 1994).

When demosponges are dissociated by squeezing them through a fine mesh, the cells have the ability to reaggre-

gate, forming a new individual (Wilson, 1907). The mechanisms underlying reaggregation have been extensively studied. The process is homeotypic and therefore of interest in relation to self and non-self discrimination in the earliest metazoa (Curtis, 1962; Moscona, 1968; McClay, 1971; Müller, 1982). Studies of newly dissociated demosponge cells shows that they exhibit rapid nondirectional crawling along the substrate (Noble and Peterson, 1972; Gaino *et al.*, 1985). Initial contacts between cells may be made by membrane bridges (Evans and Bergquist, 1974), whereas the formation of secondary aggregates is by species-specific cell adhesion molecules (Müller, 1982). Whether aggregation is brought about by cell migration or artificially, for example, by the rotary technique of Humphreys (1963), aggregates rapidly grow in size, becoming opaque under the light microscope.

In earlier work (Pavans de Cecatty, 1982), aggregates in hexactinellids, like those in demosponges, were found to form large spherical masses, and their contents could not be observed with light microscopy. In the present study, however, substrates containing sponge tissue extract or concanavalin A were used (Leys, 1995). The tissues adhere and spread out on these substrates, permitting observation of the cytoskeleton *in vitro*. The findings reported here show that, in such preparations of *Rhabdocalyptus*, tissue aggregation leads to the formation of giant syncytia in which multidirectional streaming occurs over great distances in a manner unique among the Porifera.

Materials and Methods

Specimens of *Rhabdocalyptus dawsoni* were collected by scuba from a depth of 30 m in Barkley Sound and

Saanich Inlet, British Columbia, and kept in flow-through seawater tanks at the Bamfield Marine Station and at the University of Victoria. Specimens of *Haliclona* sp. were collected intertidally at Clover Point, Victoria, British Columbia, for use in dye exchange experiments only.

Preparation of substrate

The preparation of tissue extract dried onto coverslips or plastic petri dishes, to which dissociated tissue of *R. dawsoni* adheres, is described elsewhere (Leys, 1995). Alternatively, 50 μl (100 μg $\cdot$ ml^{-1}) Concanavalin A (Con A) was pipetted onto coverslips and allowed to air dry before being used as an adhesion substrate for dissociated tissue.

Preparation of aggregates

Pieces (1 cm^3) of cleaned whole sponge tissue were squeezed through 100 μm Nitex mesh into a beaker to make 3.0–5.0 ml of dissociated tissue, then diluted to 200 ml with seawater. About 2 ml of the suspension was poured into 1.8 cm diameter plastic petri dishes containing coated coverslips and held at 11°C either by floating dishes on seawater or by placing them in an incubator. Alternatively, for video microscopy, the dissociated tissue was briefly pelleted at 1000 × g for 15 s to remove spicule debris, and the top of the pellet was pipetted onto a coated coverslip in a dish of seawater.

Computer-assisted light microscopy

Preparations were viewed with a compound microscope equipped with phase contrast and differential interference contrast (DIC) optics and with a cooling stage. Images were captured with a Panasonic digital color CCTV video camera and OMNEX digital image processor (Imagen Inc.). Photographs were taken from the screen of a Technitron television monitor.

Immunolabeling and vital staining

To prevent depolymerization of the cytoskeleton due to excess calcium, aggregates were transferred to calcium-free seawater (CFSW) for 30 min prior to fixation. For microfilament labeling, preparations were lysed at 2, 6, 12, and 24 h after plating the tissue, in a PEM buffer consisting of 50 mM piperazine-N,N'-bis[2-ethane sulfonic acid], 1 mM ethyleneglycol-bis-(β-aminoethyl ether)N,N'-tetraacetic acid, 0.5 mM MgCl$_2$ at pH 6.9 with 10% dimethylsulfoxide and 0.1% Triton X-100 for 2 min and fixed in 2% paraformaldehyde in CFSW with 10 μM EGTA and 0.04% tannic acid for 10 min. For microtubule labeling, preparations were fixed without lysing, in 2% paraformaldehyde in PEM buffer, at 30 min, 1, 6, and 12 h after plating. After one 30-min wash in 0.05 M Tris buffer pH 7.0 with 0.1% TX-100, coverslips were incu-

bated overnight in tubulin antibodies or rhodamine-phalloidin (Molecular Probes, Inc.) to visualize actin microfilaments. The tubulin antibodies used included a polyclonal anti-tubulin antibody (Chemicon); a monoclonal antibody against flagellar axonemes or isolated basal apparatus of *Polytomella* (Protista, Chlorophyceae), designated 5A6 (kindly provided by Dr. David Brown, University of Ottawa); a monoclonal antibody against yeast tubulin clone YOL1/34 (Sera Labs); a monoclonal antibody against native chick brain alpha tubulin (Amersham); and a monoclonal antibody against *Drosophila* (insect) beta tubulin, designated E7, which was developed by M. Klymkowski and obtained from the Developmental Studies Hybridoma Bank maintained by the Department of Pharmacology and Molecular Science, Johns Hopkins University School of Medicine, Baltimore, Maryland, and the Department of Biological Sciences, University of Iowa, Iowa City, Iowa. After a 30-min rinse, preparations were incubated in their respective secondary antibody for 5 h, rinsed thoroughly in phosphate buffered saline (PBS) pH 7.2, and mounted in PBS-glycerol with n-propyl gallate. To stain the nuclei, coverslips were incubated in 100 μg $\cdot$ ml^{-1} Hoechst #33342 (Sigma) for 5 min at 11°C, and immediately observed with a 40× water immersion lens. To examine the microtubule network in severed streams, a stream was cut with a scalpel while the preparation was still in a dish of seawater on an inverted microscope. After the material downstream of the wound had completely drained away, the preparation was fixed and labeled for anti-tubulin immunofluorescence as above.

Electron microscopy

For scanning electron microscopy (SEM), dissociated tissue from *Rhabdocalyptus* adhered to coverslips was transferred to CFSW for 30 min prior to fixation. Preparations were briefly lysed for 5–15 s, or fixed directly, in a fixative containing 2% glutaraldehyde, 1% OsO$_4$, 0.45 M sodium acetate buffer at pH 6.4 (Harris and Shaw, 1984), 10% sucrose and 5 μM EGTA final concentration, for 2 h on ice. Coverslips were dehydrated through a graded ethanol series, critical-point dried in CO$_2$, mounted on stubs with silver conducting paint, coated with gold in an Edwards S150B sputter coater, and examined in a JEOL JSM-35 scanning electron microscope.

For transmission electron microscopy (TEM), whole mounts were prepared on extract-coated, Formvar-coated gold grids, lysed for 2 min, and fixed as above. Whole preparations, adhered to 5 cm diameter plastic petri dishes, were acclimated to CFSW for 30 min and fixed as above. Grids were critical-point dried and viewed in a Hitachi H-7000 electron microscope. Whole preparations, fixed in plastic petri dishes, were treated with 4% hydro-

fluoric acid overnight to remove silica, dehydrated in ethanol, and embedded in Epon. For cross sections, the embedded material was taken out of the petri dish and reembedded in Epon. Thin sections were cut on a Reichert UM2 ultramicrotome and stained with uranyl acetate and lead citrate.

Pharmacological manipulations

To demonstrate the effect of various cytoskeletal disruptors on streaming, drugs (cytochalasin B, colcemid, nocodazole, Taxol, EGTA) were added to 2 ml seawater in a Falcon petri dish containing one preparation. To demonstrate reversibility of the effects, preparations were incubated in these drugs for 5 min and 2 min respectively, and transferred immediately to clean seawater every 15 min thereafter for 4.5 h. Preparations were kept at 11°C for the duration of the experiment.

Dye exchange experiments

To confirm that fusion of tissues and exchange of cytoplasm occurred during aggregation in syncytial sponges but not in cellular sponges, dissociated tissues of both sponges were loaded with fluorescent, membrane-impermeable dyes and allowed to aggregate. Dissociated tissue from both *Rhabdocalyptus* (R) and *Haliclona* (H) was briefly centrifuged at 1000 × g for 15–30 s to remove spicule and other debris. Calcein acytoxymethyl ester (CAM) and Calcein blue acytoxymethyl ester (CBAM) (Molecular Probes, Inc., Eugene, OR) were made up in DMSO to stock concentrations of 1 and 2 mM respectively. The dyes were added to the sponge tissue at a final concentration of 10 μM in microfuge tubes that were left at 10°C for 15 min. The tissue was then rinsed three times by pelleting the tissue, drawing off the remaining seawater by pipette and resuspending the pellet in fresh seawater. After the final rinse, equal volumes were plated in a 1.8-cm, extract-coated plastic petri dish as follows: (R)-CAM with (R)-CBAM; (R)-CAM with (H)-CBAM; (H)-CAM with (H)-CBAM.

Results

Fusion

Immediately after being plated, the dissociated tissues consisted of unattached rounded masses of various sizes, some of which could be identified by their collars and flagella as parts of choanoflagellate chambers. All pieces adhered to the coverslip within seconds of plating and flattened and spread out between 5 s and 10 min after plating (Fig. 2). The larger (10 μm diameter) pieces developed a broad, skirt-like lamellipodium or extended long filopodia into which the cytoplasm streamed. These adhered tissue pieces incorporated other smaller, rounded
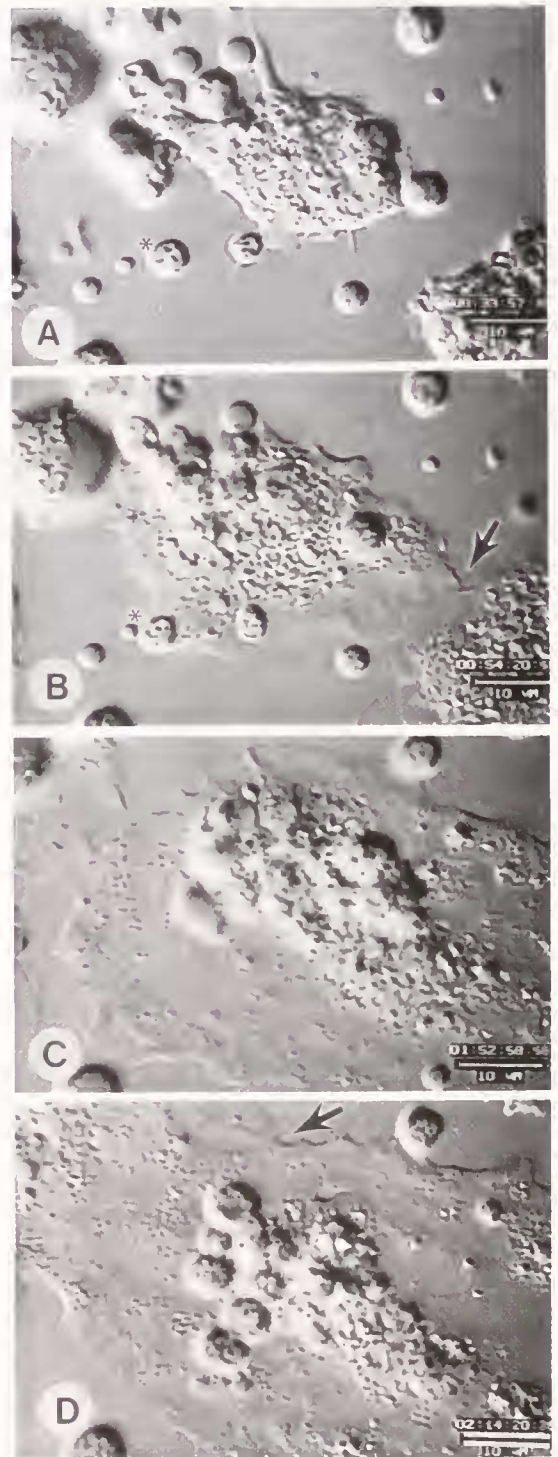

Figure 2. Fusion in adhered aggregates of *Rhabdocalyptus* taken from a video recording of tissue aggregation. Upon plating, pieces of tissue adhere and spread a skirt-like lamellipodium or long filopodia. After about 1 h of spreading, such pieces encounter each other, as shown by the overlapping lamellipodia (B, arrow). Tissues fuse and exchange cytoplasm between 5 and 30 min after first contact (C). Fused tissue pieces continue to grow in diameter, incorporating some tissue pieces (* in A and B) and fusing with others (D, arrow). Minutes after plating dissociated tissue: A, 33 min; B, 54 min; C, 102 min; D, 134 min. Bar: 10 μm. (Video available; see footnote on title page.)
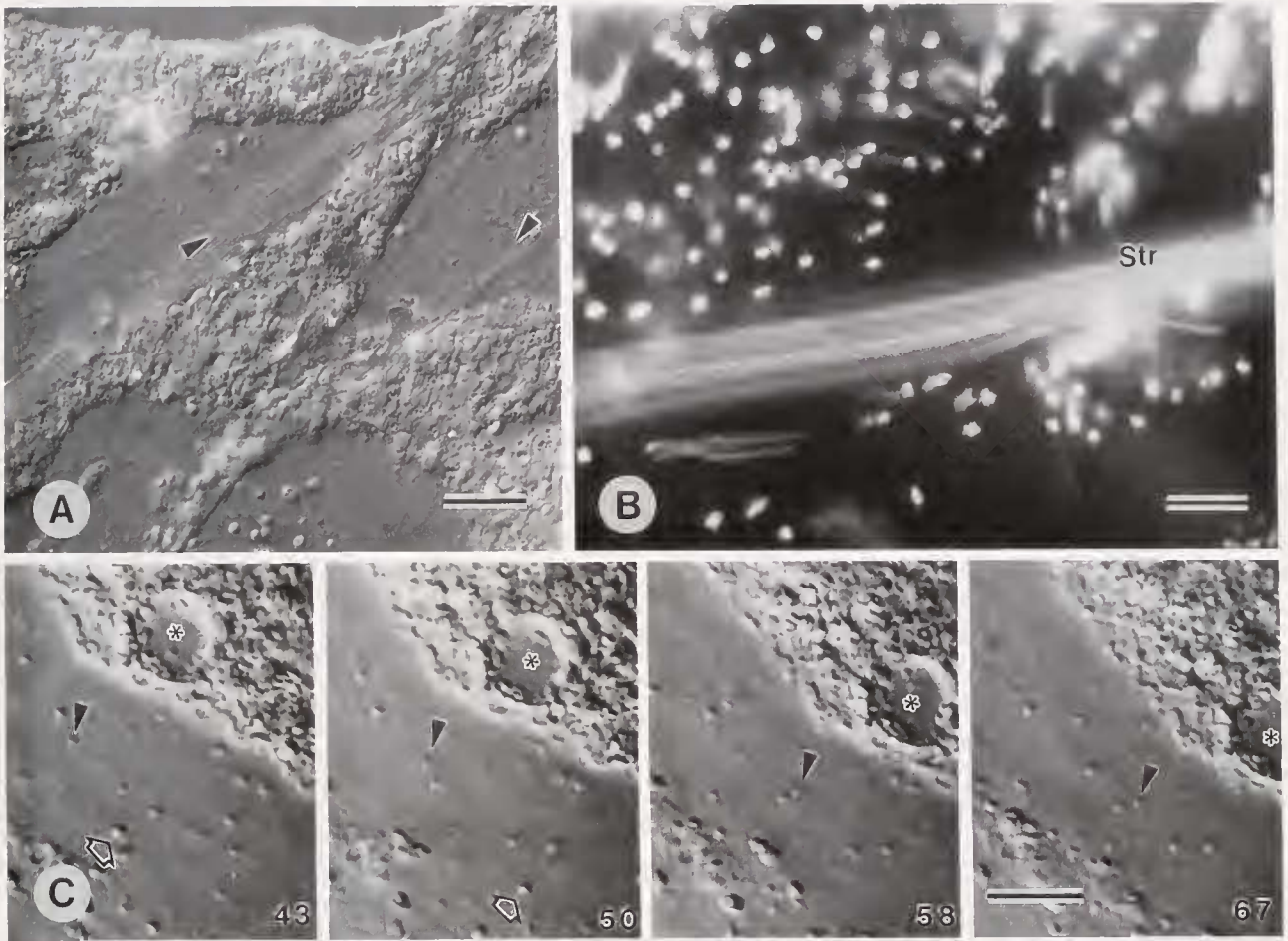
Figure 3. Twenty-four hours after plating sponge tissue, a single tissue mass covers an entire petri dish. (A) Streams (arrowheads) are abundant and run in opposite directions, winding throughout the entire coverslip. A 5-s shutter exposure allowed moving objects to leave trails. Bar: 20 μm. (B) Hoechst-labeled nuclei are visible in both streaming (STR) and stationary cytoplasm. Nuclei move in streams at just over 2 μms^{-1}. A 30-s shutter exposure causes all moving nuclei to leave a trail of light marking their path. Bar: 20 μm. (C) Images from a video monitor showing bulk transport of material in streams (*) beside organelles that are being transported individually (arrow and arrowhead). Streams move continuously but at a slower rate than individual organelles. The organelle marked by an open arrow moves steadily, leaving the field of view in the third frame, while the organelle marked by an arrowhead moves haltingly and eventually stops. Frames shown are at 8-s intervals. Bar: 10 μm. (Video available; see footnote on title page.)

pieces of tissue by drawing them in to a central location within the aggregate. Independent adhered pieces encountered each other by way of the lamellipodia or filopodia. Fusion did not always occur immediately upon contact of lamellipodia. Lamellipodia even overlapped one another for 10–30 min before the exchange of organelles could be clearly detected (Fig. 2b, 54 min). A clear sign of fusion, however, was a shared lamellipodium at the point of touching, followed by exchange of organelles. Within minutes of fusion there was no evidence that the single piece of tissue had been otherwise. Lamellipodial extension continued in all directions, and streams of cytoplasm started to become clearly visible circumnavigating

the aggregate in both directions. Fusion continued with other tissue pieces that were encountered.

Cytoplasmic streaming

As aggregates increased in size by incorporating neighboring tissue masses, organelle movement became organized into wider and straighter streams, until eventually the entire coverslip was covered in tissue that consisted of dramatic rivers of flowing cytoplasm traversing the coverslip, sometimes running parallel in opposite directions (Fig. 3a) and even crossing each other without apparent interruption in volume or velocity of flow. Streams
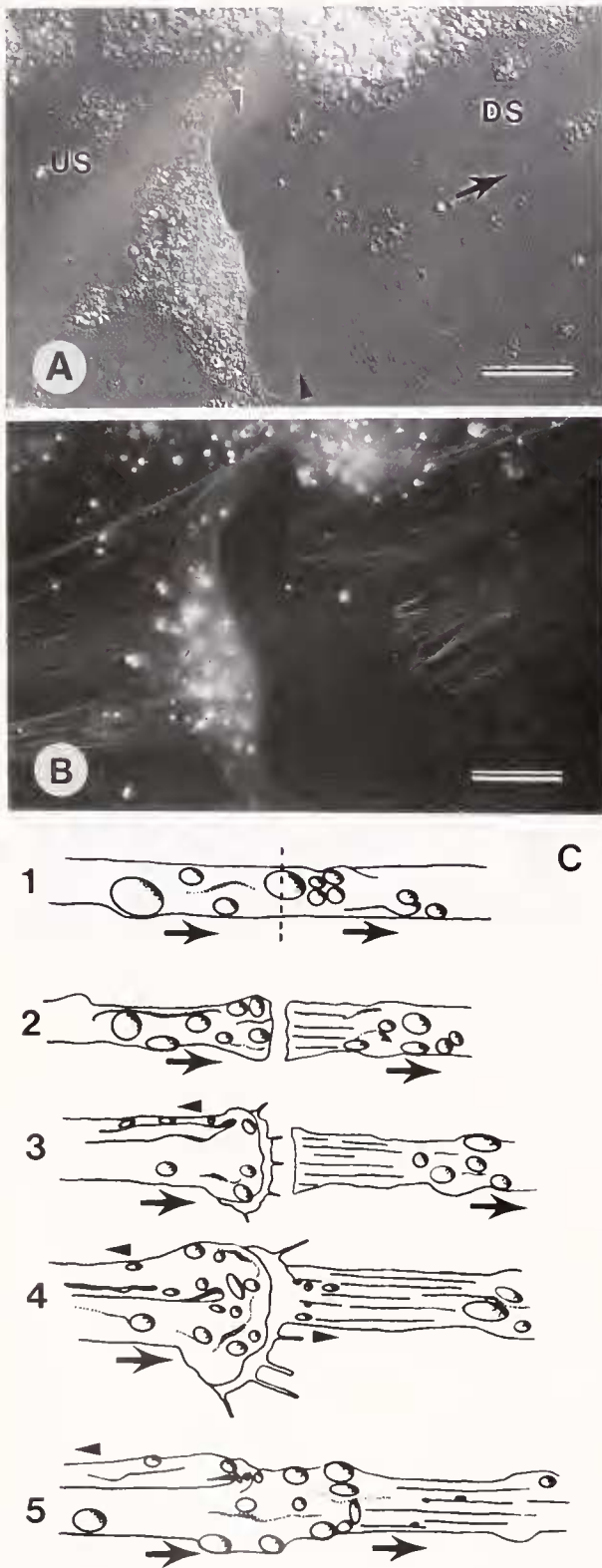
of cytoplasm flowed uninterrupted for distances up to several centimeters, limited only by the area of coated substrate available. Large streams continually changed direction and both gained and lost volume. Under DIC microscopy, bulk cytoplasm in streams could be seen to contain spicule debris and vesicles of various sizes. With electron microscopy, cytoplasm fixed while it was streaming showed similar objects along with numerous mitochondria, nuclei, Golgi bodies, and some archaeocytes. Fluorescent staining with Hoechst #33342 showed nuclei in both the flowing and stationary cytoplasm (Fig. 3b). Individual nuclei could be followed in streams for distances up to several millimeters.

Organelles resolvable by video-enhanced contrast microscopy in thin areas of tissue moved at an average rate of $2.15 \pm 0.33\ \mu m \cdot s^{-1}$ ($n = 100$), while bulk streams moved at an average rate of $1.72 \pm 0.30\ \mu m \cdot s^{-1}$ ($n = 100$) (Fig. 3c). However, some organelles moved haltingly, sometimes reversing direction or apparently bumping into each other; these organelles seemed to buckle or bend as they reversed. Organelles moving in broad lamellipodia followed no one direction, and occasionally paused for some seconds. In some streams the bulk cytoplasm that had been flowing diminished in volume to isolated organelles, to be followed once again by bulk cytoplasm.

Cutting a stream with a scalpel caused cytoplasm to build up on the upstream side of the wound. Downstream of the wound, cytoplasm continued to flow away until no movements of organelles could be detected, but birefringent tracks could still be seen by phase contrast and DIC microscopy (Fig. 4a). Immunofluorescence of tubulin on the depleted side showed that microtubule bundles remained, even though all streaming along them had ceased (Fig. 4b). Eventually the cytoplasm upstream of the wound began to turn back upon itself, initiating a new stream parallel to the original one but in the reverse direction. At the same time, lamellipodial and filopodial processes were extended toward the downstream side until, after several minutes, contact was once again made, followed by fusion; a few organelles, soon followed by the full stream, then began to flow along the original track. These stages are summed up diagrammatically in Figure 4c.

With time, the tissue amassed in central locations and gradually withdrew from the substrate until an opaque

Bar: 30 μm. (B) Anti-tubulin labeling of microtubules in the wounded stream. Microtubules remain, even though all visible organelle movement has ceased downstream of the wound. Bar: 30 μm. (C) Diagram illustrating the sequence of events after wounding a stream. The cut cytoplasm, represented by the dashed line in (1), builds up on the upstream side (2), eventually forging a new path in the reverse direction (3), as indicated by arrowheads. Filopodial and lamellipodial projections extend across the wound, making contact with the original tracks (4). Single organelles, rapidly followed by the bulk cytoplasm, begin to stream along the former path (4). Arrows indicate direction of flow.
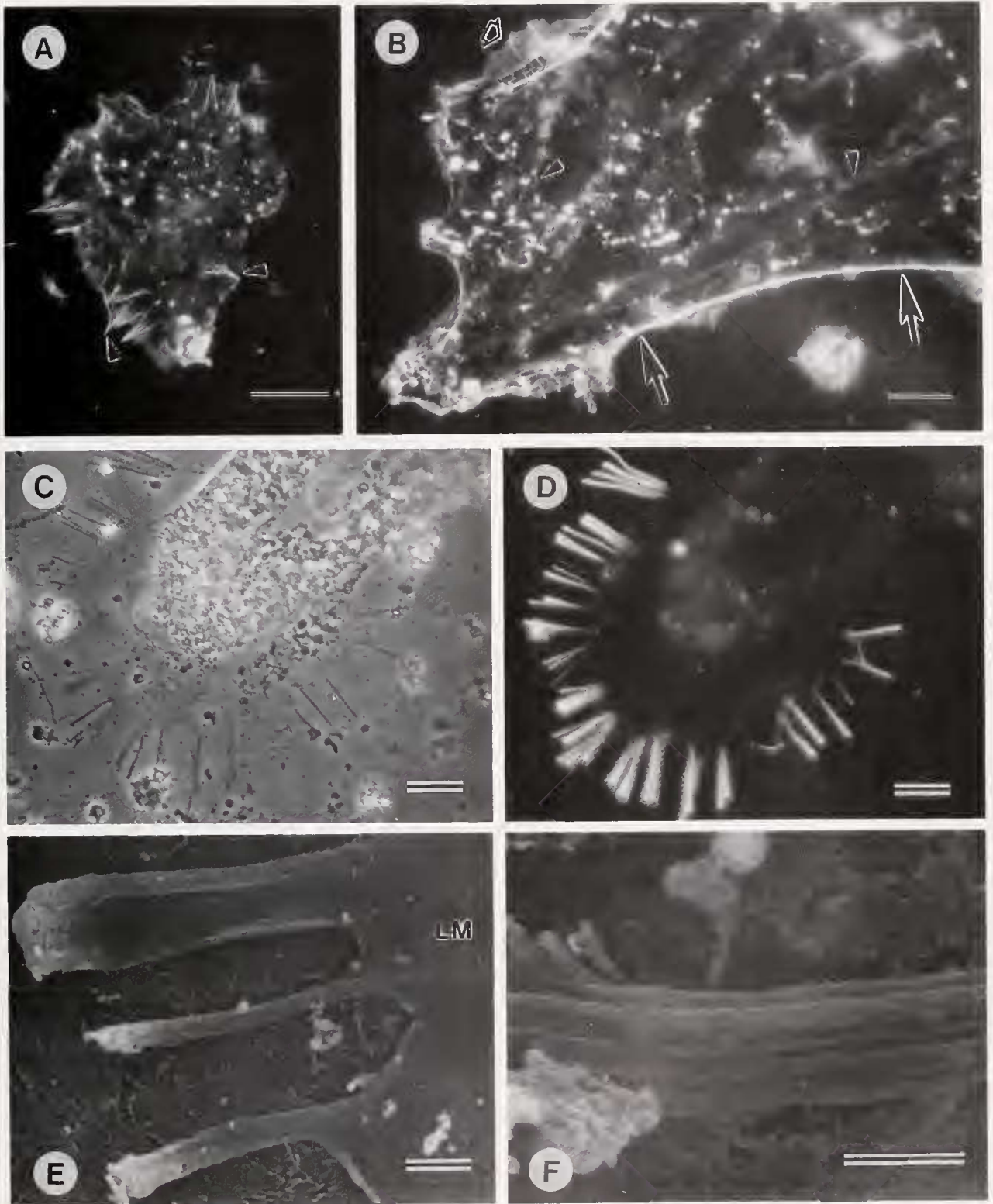
Figure 4.   The effect of severing streams of cytoplasm. (A) When cut, the cytoplasm downstream (DS) of the wound (arrowhead) continues to drain in the direction of the arrow, while that upstream (US), builds up.

Figure 5. The actin cytoskeleton in adhered aggregates after lysing. (A) Rhodamine-phalloidin labeling of aggregates 2 h after plating reveals tissue masses 30–100 µm in diameter that possess well-defined rods projecting from their periphery (arrowheads). Bar: 20 µm. (B) Six hours after plating dissociated tissue, aggregates are already 0.5 mm in length and can be much larger. A portion of a fused aggregate shows giant

sphere was formed. Such spheres could temporarily adhere once again if new substrate was offered.

The actin cytoskeleton

Only by briefly lysing preparations before fixation was it possible to obtain a clear picture of actin distribution in adhered tissue preparations. Attempts to label microfilaments with a polyclonal antibody to actin and with rhodamine-phalloidin in whole preparations gave, at best, weak labeling of microfilament bundles whose precise location could not be determined. However, lysing the tissue for 5 s–2 min resulted in detachment of the superficial part of the tissue mass, exposing the layer adjacent to the substrate in which actin labeling produced clearer results.

Two hours after plating, aggregates were 30–100 μm in diameter and possessed blunt rods containing thick actin bundles that projected from the periphery (Fig. 5a). The edges of large lamellipodia labeled strongly with rhodamine-phalloidin and stress fibers some 20 μm in length transected the tissue. After 6 h, these masses had joined, and no membranes demarcating cell boundaries could be seen within the tissue mass by phase-contrast microscopy. Rhodamine-phalloidin–labeled microfilament bundles up to several hundred micrometers long were observed to run around the edges of adhered aggregates (Fig. 5b). A network of fine filaments was apparent beneath the stress fibers throughout the syncytium. One-day-old adhered aggregates showed no change in general morphology or in actin distribution, although the distances over which bundles of microfilaments could be followed now exceeded 500 μm. After 24 h, much of the tissue had been drawn into central, opaque areas. The edges of such dense tissue masses possessed blunt rod-like extensions reaching some 18.0 ± 4.5 μm ($n = 20$) out from the edge of the lamellipodium, forming a "hairbrush effect" (Fig. 5c). These extensions labeled very strongly for actin (Fig. 5d). The organization of actin in aggregates older than 48 h did not change significantly, because most tissue was centralized at that time, anchored firmly by massive projections from the edges. Scanning electron microscopy of the giant rods in intact and lysed preparations revealed thick actin bundles forming their core (Fig. 5e, f).

The microtubule cytoskeleton

Preservation of microtubules required the use of a special fixation method (see *Immunolabeling and vital staining* in the Materials and Methods), after which it was possible to visualize microtubule bundles by phase contrast and immunofluorescence microscopy. These bundles were still visible after cytochalasin B treatment, but not after treatment with nocodazole or colcemid. Of five anti-tubulin antibodies, only two monoclonal antibodies—one prepared against beta tubulin in *Drosophila* and the other against chick brain alpha tubulin—gave good immunofluorescence in whole mounts. Control experiments showed that all antibodies labeled microtubules in neurons and cilia of tunicate branchial basket and veliger larvae.

Immunofluorescence microscopy revealed a remarkable change in the microtubule network over the course of aggregation. At 30 min, microtubules formed a fine meshwork in tissue pieces up to 80 μm in diameter; microtubules appeared delicate, some directly crossing and others winding around the tissue mass. Nuclei appeared randomly scattered among the microtubules. After 6 h, the microtubules were already well organized into striking bundles, many of which traversed an entire coverslip (Fig. 6a). Where many bundles of microtubules converged into one path they became rigidly straight (Fig. 6b). At the edge of preparations, the entire bundle gave way to a reticular network of lines (Fig. 6c). These often wound through giant lamellipodia before joining the main stream and traversing the coverslip again.

Double labeling of actin and tubulin proved unsatisfactory because the lysing procedure required for clear visualization of the microfilament network usually destroyed the continuity of microtubules. However, double labeling of nuclei and microtubules clearly demonstrated that nuclei were randomly distributed among microtubules (Fig. 8f).

The microtubules were difficult to fix for electron microscopy. The fixative used by Mackie and Singla (1983) does not stabilize microtubules except in flagella. The fixative of Harris and Shaw (1984) gave excellent results for both general ultrastructure and microtubule preservation. In cross sections of the adhered tissue, microtubules were seen both in bundles and lying individually (Fig. 7a and inset). In thicker areas of the tissue, large bundles were seen at the surface of the preparation as well as through the depth of the tissue. Rarely in these areas did they occur singly, and rarely were they on the bottom of thick tissue masses. In horizontal section, microtubule bundles could be traced for many hundreds of micrometers (Fig.

bundles of microfilaments delineating the border (filled arrows). A network of microfilament bundles traverses the basal layer adjacent to the substrate (arrowheads) and small, actin-dense rods lie within lamellipodia (open arrow). Bar: 20 μm. (C, D) Adhered aggregates older than 12 h possess giant rods projecting from the periphery as a "hairbrush" (C: phase contrast; D: rhodamine-phalloidin labeling of unlysed tissue.) Bar: 10 μm. (E) SEM shows several giant rods extending from the lamellipodium (LM). (F) High magnification SEM of a lysed actin-dense rod. E, F, bar: 0.5 μm.
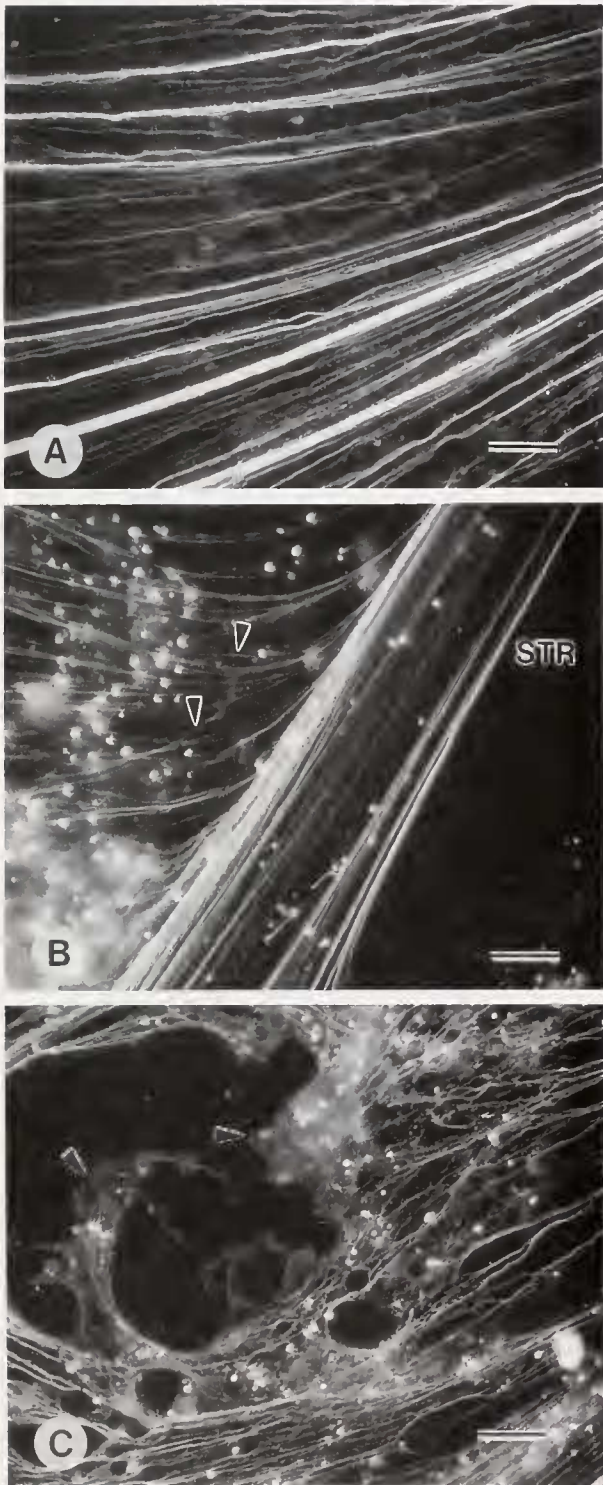
Figure 6. Immunofluorescence of the microtubule cytoskeleton in adhered aggregates. (A) Six hours after plating, microtubule bundles already stretch up to a centimeter across an entire coverslip. A–C, bar: 20 μm. (B) Microtubule bundles are rigidly straight (STR) in streams, while those leaving or converging on a stream (arrowheads) are often curved. (C) At the edges of preparations, bundles give way to a fine meshwork of microtubules that reach into lamellipodia (arrowheads).

7b). Nuclei, mitochondria, coated vesicles, and tubulo-vesicular organelles were all found adjacent to microtubule bundles as well as lying free in the cytosol. Tracts of microtubules ran beside, but not through, clusters of archaeocytes and spherulous cells. In whole mounts of aggregates adhered to tissue extract on Formvar-coated gold EM grids, organelles of various sizes were also seen associated with linear structures with diameters of approximately 22 nm, presumably microtubules (Fig. 7c).

Inhibition experiments

Organelle movement was reversibly inhibited by both nocodazole and colcemid but was unaffected by cytochalasin B (Table I), although the latter caused the tissue to detach from the substrate. Neither Taxol nor 10 μM EGTA had any effect on rate of organelle transport.

Dye exchange

Attempts to inject the fluorescent dyes carboxyfluorescein or lucifer yellow through glass capillary microelectrodes were not successful because of difficulty in obtaining stable penetrations. The surface membrane of adhered aggregates either blocked the electrode or did not reseal around the electrode after penetration. However, fluorescent dyes coupled to acytoxymethyl esters such as Calcein AM (CAM) and Calcein blue AM (CBAM) could be readily loaded into dissociated tissue. Tissue loaded with CAM plated in the same culture dish with tissue loaded with CBAM produced fused aggregates in which streaming occurred. After 6–12 hours, these aggregates were uniformly blue-green (Fig. 8a, b, c). In control experiments in which dissociated tissue from the cellular sponge *Haliclona permolis* loaded with CAM was plated with tissue from *Rhabdocalyptus* loaded with CBAM, *Haliclona* cells rapidly formed large round aggregates, did not mix with *Rhabdocalyptus* tissue, and did not take up the blue dye (Fig. 8d). *Haliclona* tissue, even if adhered, showed no sign of cytoplasmic streaming. When two samples of *Haliclona* tissue were loaded with CAM and CBAM respectively and plated together, there was no exchange of dye, although after 12 h aggregates were mosaics of both colors (Fig. 8e).

Discussion

This remarkable preparation provides the first evidence of fusion during aggregation of dissociated hexactinellid sponge tissues and reveals an entirely novel form of cytoplasmic streaming. It further reveals a cytoskeletal framework that is unique in the histology of sponges and, perhaps, the entire metazoa, for sheer size. Given the evidence of syncytialization in other hexactinellids, streaming may be widespread within the group. The syncytial
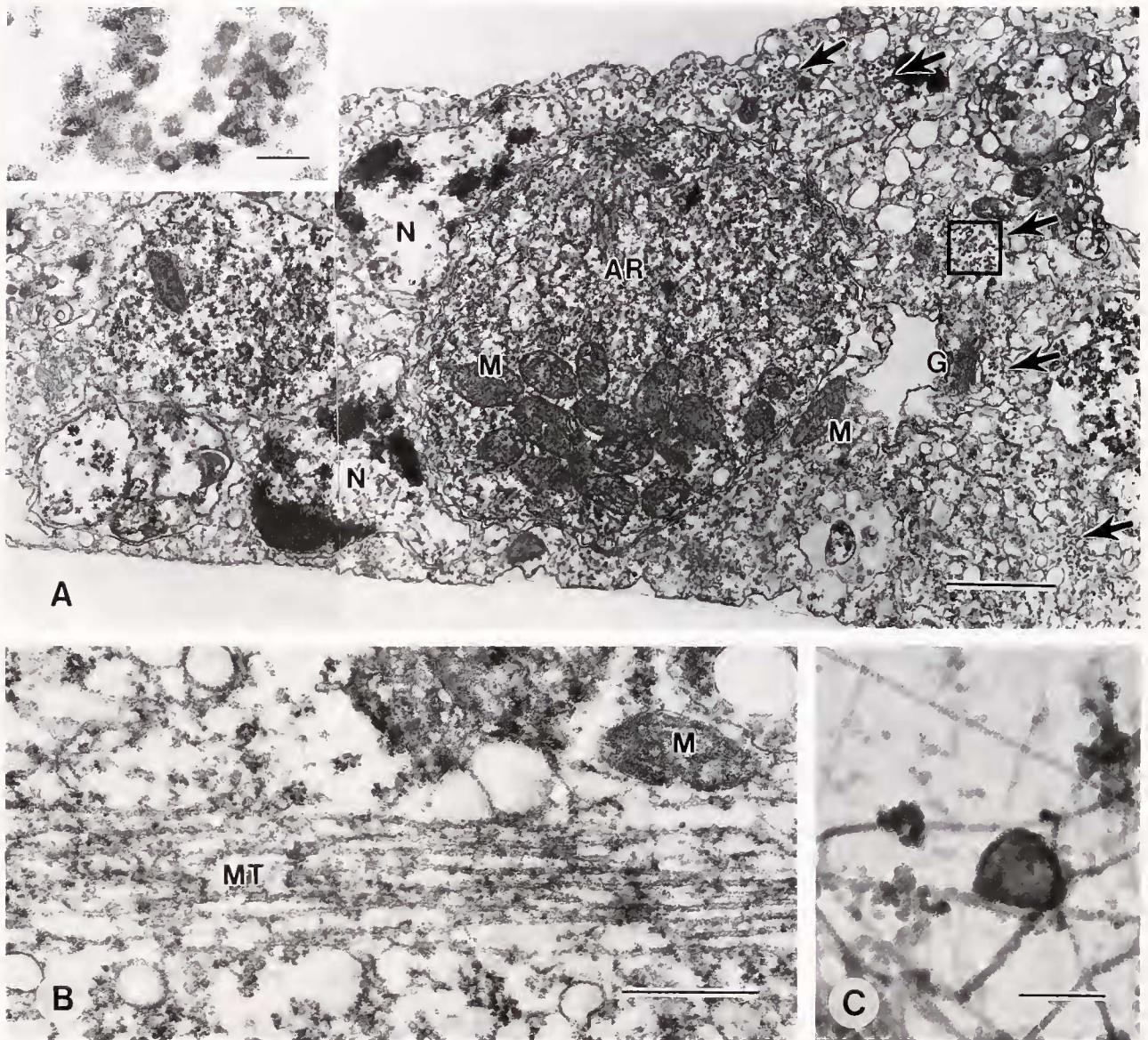
Figure 7.   Electron microscopy of adhered aggregates. (A) In cross section, cellular components (such as archaeocytes) lie within the multinucleated cytoplasm, which is surrounded above and below by a continuous membrane. Microtubule bundles lie at the surface of streams and throughout the tissue (arrows). Bar: 1 μm. Inset shows an enlargement of microtubules from within the box. Bar: 0.1 μm. Nuclei, N; archaeocyte, AR; Golgi, G; mitochondria, M. (B) Horizontal section through a stream showing a bundle of microtubules (MT) with associated organelles. Bar: 0.5 μm. (C) A whole-mount preparation showing an organelle associated with linear structures. Bar: 0.2 μm.

condition of hexactinellid sponges appears to be significant in two ways. First, syncytialization would allow the transport of nutrients throughout the animal in the absence of mobile archaeocytes (Mackie and Singla, 1983). The present findings suggest that cytoplasmic streams may be the transport routes. Second, the lack of membrane barriers within the syncytium presumably makes possible the propagation of impulses coordinating flagellar arrests

(Lawn *et al.*, 1981; Mackie *et al.*, 1983). Cellular sponges, lacking nerves and gap junctions, have no such capability.

Formation of a syncytium

Membrane fusion is the means by which *Rhabdocalyptus* forms a syncytium during aggregation. Nonetheless, not all tissue components fuse. Small rounded pieces of tissue, which do not form lamellipodia, are drawn into

Table I

The effect of cytoskeletal disruptors and stabilizers on transport in Rhabdocalyptus dawsoni

Drug	Action	Effect on streaming
Colcemid (10 μg/ml)	Depolymerizes	Stops streaming
Nocodazole (1 μg/ml)	Depolymerizes	Stops streaming
Taxol (10 μg/ml)	Stabilizes MTs	No effect
EGTA (10 μM)	Chelates calcium	No effect

MTs, microtubules; MFs, microfilaments.

the center of larger aggregates that are fusion products. Whether syncytia can be formed by fusion of tissues from two species of hexactinellids has not yet been tested. The observation of dye spread following fusion in *Rhabdocalyptus* confirms the syncytial state of the tissues of this sponge, in contrast to *Haliclona*, where no dye spread was observed during aggregation. Failure of dye to spread within *Haliclona* might be due to inability of Calcein to pass through gap junctions or to the absence of gap junctions or other aqueous intercellular pathways (see Mackie, 1984).

Streaming

Before the first fusion event, organelles appear to move in adhered tissue pieces in the way described for other cells, including basal epithelial cells of freshwater sponges (Wachtmann and Stockem, 1992). After fusion, however, streaming in *Rhabdocalyptus* aggregates takes on characteristics unlike any transport mechanism previously described. For example, streams maintain neither a constant volume nor a single direction. Flow may reverse direction, albeit with a slight decrease in rate at the point of turning. And there is no limit to the length of streams. The closest parallel to this system is the streaming of bulk cytoplasm and individual organelles in reticulopodia of the protists *Allogromia* and *Reticulomyxa* (Travis and Allen, 1981; Koonce *et al.*, 1986), and there may be parallels with bulk cytoplasmic flow in characean algae, where a mechanism for coupling of bulk cytoplasm to microfilament bundles by means of the endoplasmic reticulum has been described (Kachar and Reese, 1988).

Rates of organelle transport in *Rhabdocalyptus* are within the range reported for fast axoplasmic transport (Allen *et al.*, 1982) and other systems involving microtubule-associated motors. The prominence of the network of microtubule bundles and the inhibition of streaming by colcemid and nocodazole, drugs that depolymerize microtubules, strongly implicate the microtubules as the transport pathway, making it likely that microtubule-associated motor proteins are involved. A recent account of cell shape changes in newly hatched freshwater sponges

and sandwich cultures of marine sponges showed that these sponge cells are capable of movement at rates of up to 15 $\mu m \cdot min^{-1}$ (Bond, 1992). Lamellipodial movements in *Rhabdocalyptus* aggregates appear to occur at about the same rate. However, the transport of nuclei and other organelles in streaming cytoplasm at seven to ten times that rate suggests that the two mechanisms of movement are different.

The effects of cutting cytoplasmic streams in *Rhabdocalyptus* are reminiscent of the effects of ligaturing axons (Weiss and Hiscoe, 1948). Streams, when cut, build up on the upstream side and drain on the downstream side. Furthermore, the lamellipodium that extends in search of the lost distal stump greatly resembles a nerve growth cone. Nonetheless, although streams may run in opposite directions beside or above one another, there is no evidence of the bidirectional flow within the same stream or along the same microtubule that may occur in axons. Further work with a perfused, reactivated sponge preparation will help to determine the precise mechanism of transport.

Cytoskeletal architecture

One of the most exciting findings of this study is the vast cytoskeletal framework of the adhered aggregates. The lengths of both microfilament and microtubule bundles are of proportions unheard of in any other tissue. Figure 9 presents a three-dimensional summary diagram of the cytoskeletal architecture in a stream at the edge of an adhered preparation, showing the relationship between cytoplasmic organelles and microtubules.

It is tempting to infer from the difficulty of fixing and labeling microtubules that, as in *Reticulomyxa* (Koonce *et al.*, 1986), tubulin in lower eukaryotes differs significantly from mammalian tubulin, or that bundling somehow interferes with antibody recognition. The composition of microtubules, sites of microtubule nucleation, and microtubule polarity are topics that merit further study in this sponge.

Filopodia containing dense actin cores have been reported in aggregating cells from cellular sponges (Burlando *et al.*, 1984; Gaino and Burlando, 1985), suggesting functional similarities. However, the stiff, actin-filled extensions that form a "hairbrush" effect in older adhered aggregates are unique. These enormous processes are implicated in the adhesion of aggregates because some areas could be found where the tissue had detached, leaving the "hairbrush" attached.

Adhered aggregates as a model of whole sponges

The difficulty of visualizing cytoplasmic movements in intact sponges makes it hard to say if processes similar to those seen in cultured aggregates are going on. Neverthe-
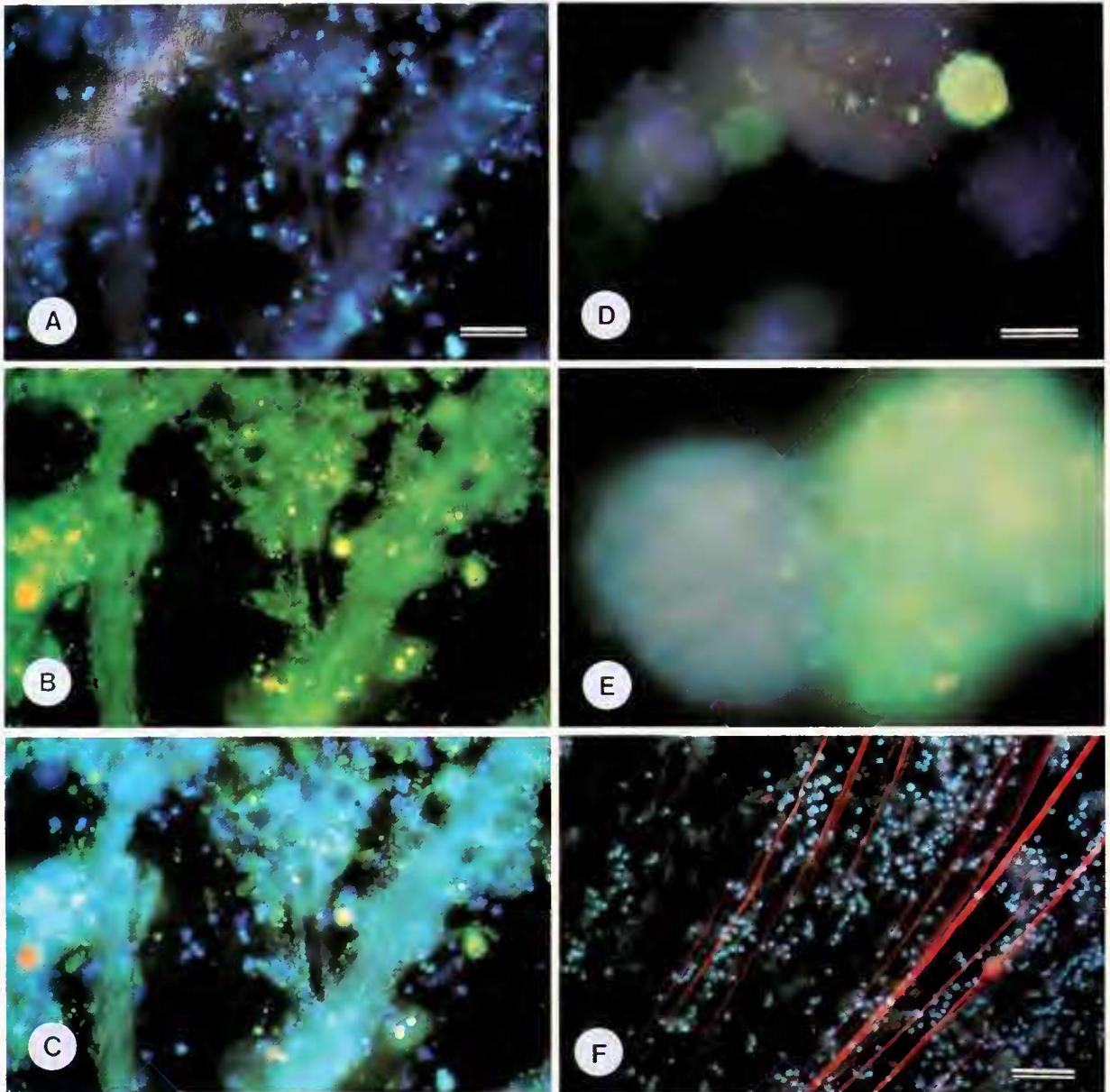
Figure 8. Demonstration of syncytial tissues in *Rhabdocalyptus* (A–C) Spread of dye in aggregates. *Rhabdocalyptus* tissue loaded separately with Calcein AM and Calcein blue AM and plated together fuses to allow blue dye throughout (a) and green dye throughout (b); thus a double exposure shows a blend of the two colors (C). A–C, bar: 25 μm. (D) *Rhabdocalyptus* tissue loaded with Calcein AM (green) and plated with tissue from the cellular sponge *Haliclona* loaded with Calcein blue AM (blue) shows that neither dye was membrane permeable once loaded, because neither sponge incorporated the other dye. Although both small and large round aggregates of *Rhabdocalyptus* have adhered to the larger *Haliclona* aggregate, no exchange of dye occurs. D, E, bar: 50 μm. (E) Tissue from *Haliclona* loaded separately with Calcein AM and Calcein blue AM and plated together did not exchange dye after 12 h, although aggregates often consisted of mosaics of both colors, as shown by a double exposure. (F) Double labeling of microtubules (red) and nuclei (blue) in day-old adhered aggregates of *Rhabdocalyptus dawsoni* demonstrates that the tissue is multinucleate. Bar: 25 μm.
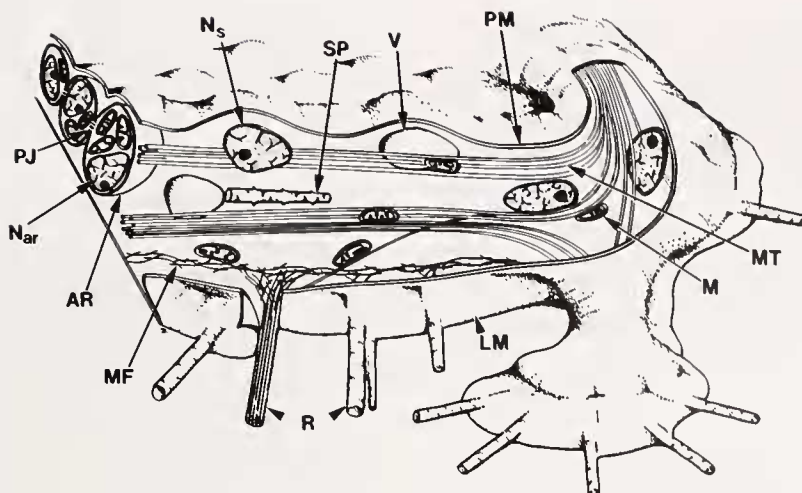
Figure 9. An illustration summarizing the cytoskeletal architecture in a 24-h adhered aggregate of *Rhabdocalyptus*. Microfilament bundles (MF) traverse the basal layer of aggregates. At the periphery, microfilament bundles give rise to giant actin-dense rods (R), which extend through lamellipodia (LM) to anchor the preparation to the substrate. Inside a cutaway of the plasma membrane (PM), a stream is exposed showing bundles of microtubules (MT) with associated nuclei (N_s), mitochondria (M), and vesicles (V). Also adjacent to the microtubules are groups of archaeocytes (AR), with their own nuclei (N_{ar}), connected to each other and the rest of the cytoplasm by perforate plugged junctions (PJ).

less, the likelihood that streaming occurs in the intact sponge is borne out by observations of streaming in regenerating fragments of the whole animal (Leys and Mackie, 1994). Video microscopy of aggregates suggests that streaming, or the microtubule network involved in streaming, may play a role in organizing the tissues of intact sponges, for instance by influencing the distribution and clustering of archaeocytes, spherulous cells, choanoblasts, and collar bodies. Archaeocytes do not appear to play the central role during aggregation in *Rhabdocalyptus* that they do in cellular sponges (Buscema *et al.*, 1980). Because adults of this species can be up to 2 m in length, and assuming that the trabecular tissues are continuous throughout the animal, *Rhabdocalyptus* must represent one of the largest syncytial organisms within the metazoa.

The evidence presented in this paper shows that adhered aggregates of *Rhabdocalyptus* possess a unique cellular motile system and a giant cytoskeleton. The observations strongly support the view that most of the cytoplasm in hexactinellids constitutes a multinucleate syncytium. It now seems clear that hexactinellids differ substantially from cellular sponges and should be differentiated from them at a high taxonomic level (Bergquist, 1978), as reflected in the subphyla Symplasma and Cellularia proposed by Reiswig and Mackie (1983).

Acknowledgments

Literature Cited

Allen, R. D., J. Metuzals, I. Tasaki, S. T. Brady, and S. P. Gilbert. 1982. Fast axonal transport in squid giant axon. *Science* **218**: 1127–1128.

Bergquist, P. R. 1978. *Sponges*. Hutchinson and Co., London.

Bond, C. 1992. Continuous cell movements rearrange anatomical structures in intact sponges. *J. Exp. Zool.* **263**: 284–302.

Boury-Esnault, N., and J. Vacelet. 1994. Preliminary studies on the organization and development of a hexactinellid sponge from a Mediterranean cave, *Oopsacas minuta*. Pp. 407–416 in *Sponges in Time and Space. Proc. 4th Int. Porifera Congress*, R. W. M. van Soest, T. M. G. van Kempen, and J. Braekman, eds. A. A. Balkema, Rotterdam.

Burlando, B., E. Gaino, and P. C. Marchisio. 1984. Actin and tubulin in dissociated sponge cells. Evidence for peculiar actin containing microextensions. *E. J. Cell Biol.* **35**: 317–321.

Buscema, M., D. De Sutter, and G. Van de Vyver. 1980. Ultrastructural study of differentiation processes during aggregation of purified sponge archaeocytes. *Wilhelm Roux's Archives* **188**: 45–53.

Curtis, A. S. G. 1962. Pattern and mechanism in the reaggregation of sponges. *Nature* **196**: 245–248.

Evans, C. W., and P. R. Bergquist. 1974.   Initial cell contact in sponge aggregates. *J. Microsc* 21: 185–188.

Gaino, E., and B. Burlando. 1985.   Cytoskeleton and morphology of dissociated sponge cells. A whole mount and scanning electron microscopic study. *Eur. J Cell Biol.* 39: 328–332.

Gaino, E., L. Zunino, B. Burlando, and M. Sara. 1985.   The locomotion of dissociated sponge cells: a cell-by-cell, time-lapse film analysis. *Cell Motil.* 5: 463–474.

Harris, P., and G. Shaw. 1984.   Intermediate filaments, microtubules and microfilaments in epidermis of sea urchin tube feet. *Cell Tissue Res.* 236: 27–33.

Humphreys, T. 1963.   Chemical dissolution and *in vitro* reconstruction of sponge cell adhesions. 1. Isolation and functional demonstration of the components involved. *Dev. Biol.* 8: 27–47.

Hyman, L. H. 1940.   *The Invertebrates.* Vol. 1, McGraw-Hill, New York.

Ijima, I. 1901.   Studies on the Hexactinellida. Contribution I (Euplectellidae). *J. Coll. Sci. imp. Univ. Tokyo* 15: 1–299.

Kachar, B., and T. S. Reese. 1988.   The mechanism of cytoplasmic streaming in characean algal cells: sliding of endoplasmic reticulum along actin filaments. *J. Cell Biol.* 106: 1545–1552.

Koonce, M. P., U. Euteneuer, K. L. McDonald, D. Menzel, and M. Schliwa. 1986.   Cytoskeletal architecture and motility in a giant freshwater amoeba. *Cell Motil. Cytoskeleton* 6: 521–533.

Lawn, I. D., G. O. Mackie, and C. L. Singla. 1981.   Conduction system in a sponge. *Science* 211: 1169–1171.

Leys, S. P. 1995.   Sponge cell culture: use of a native tissue extract as a culture substrate. *In Vitro Cell. Dev. Biol. Animal.* (in press).

Leys, S. P., and G. O. Mackie. 1994.   Cytoplasmic streaming in the hexactinellid sponge *Rhabdocalyptus dawsoni* (Lambe 1873). Pp. 417–423 in *Sponges in Time and Space. Proc. 4th Int. Porifera Congress,* R. W. M. van Soest, T. M. G. van Kempen, and J. Braekman, eds. A. A. Balkema, Rotterdam.

Mackie, G. O. 1981.   Plugged syncytial interconnections in hexactinellid sponges. *J. Cell Biol.* 91: 103a.

Mackie, G. O. 1984.   Introduction to the diploplastic level. Pp. 43–46 in *Biology of the Integument,* Vol. 1: Invertebrates, J. Bereiter-Hahn, A. G. Matoltsy, and K. S. Richards, eds. Springer-Verlag, Berlin.

Mackie, G. O., and C. L. Singla. 1983.   Studies on hexactinellid sponges. I. Histology of *R. dawsoni* (Lambe 1873). *Phil. Trans. Royal Soc. Lond. B* 301: 365–400.

Mackie, G. O., I. D. Lawn, and M. Pavans de Ceccatty. 1983.   Studies on hexactinellid sponges. II. Excitability, conduction and coordination of responses in *Rhabdocalyptus dawsoni* (Lambe, 1873). *Phil. Trans. R. Soc. Lond. B* 301: 401–418.

McClay, D. R. 1971.   An autoradiographic analysis of the species specificity during sponge cell reaggregation. *Biol. Bull.* 141: 319–330.

Moscona, A. A. 1968.   Cell aggregation: properties of specific cell-ligands and their role in the formation of multicellular systems. *Dev. Biol.* 18: 250–277.

Muller, W. E. G. 1982.   Cell membranes in sponges. *Int. Rev. Cytol.* 77: 129–181.

Noble, P. B., and S. C. Peterson. 1972.   A two-dimensional random-walk analysis of aggregating sponge cells prior to cell contact. *Exp. Cell Res.* 75: 288–290.

Pavans de Ceccatty, M. 1982.   *In vitro* aggregation of syncytia and cells of a Hexactinellida sponge. *Dev. Comp. Immunol.* 6: 15–22.

Reiswig, H. M. 1979.   Histology of Hexactinellida (Porifera). *Colloq. Int. Cent. Natn. Res. Scient.* 291: 173–180.

Reiswig, H. M. 1991.   New perspectives on the hexactinellid genus *Dactylocalyx* Stutchbury. Pp. 7–20 in *Fossil and Recent Sponges,* J. Reitner and H. Keupp, eds. Springer, Berlin.

Reiswig, H. M., and G. O. Mackie. 1983.   Studies on hexactinellid sponges. III. The taxonomic status of Hexactinellida within the Porifera. *Phil. Trans. R. Soc. Lond. B* 301: 419–428.

Schultz, F. E. 1887.   Report on the hexactinellida collected by H.M.S. *Challenger* during the years 1873–1876. *Rep. Sci. Res. Challenger Zool.* 21: 1–513.

Travis, J. L., and R. D. Allen. 1981.   Studies on the motility of the foraminifera. I Ultrastructure of the reticulopodial network of *Allogromia laticollaris* (Arnold). *J. Cell Biol.* 90: 211–221.

Wachtmann, D., and W. Stockem. 1992.   Microtubule- and microfilament-based dynamic activities of the endoplasmic reticulum and the cell surface in epithelial cells of *Spongilla lacustris* (Porifera, Songillidae). *Zoomorphology* 112: 117–124.

Weiss, P., and H. B. Hiscoe. 1948.   Experiments on the mechanism of nerve growth. *J. Exp. Zool.* 107: 315–396.

Wilson, H. V. 1907.   On some phenomena of coalescence and regeneration in sponges. *J. Exp. Zool.* 5: 245–258.